

Received May 25, 2019, accepted June 25, 2019, date of publication July 8, 2019, date of current version July 26, 2019.

Digital Object Identifier 10.1109/ACCESS.2019.2927121

Multivariate Pattern Analysis of EEG-Based Functional Connectivity: A Study on the Identification of Depression

HONG PENG¹, (Member, IEEE), CHEN XIA¹, ZIHAN WANG¹, JING ZHU¹, XIN ZHANG¹, SHUTING SUN¹, JIANXIU LI¹, XIAONING HUO², AND XIAOWEI LI¹, (Member, IEEE)

¹Gansu Provincial Key Laboratory of Wearable Computing, School of Information Science and Engineering, Lanzhou University, Lanzhou 730000, China

²The Third People's Hospital of Lanzhou, Lanzhou 730000, China

Corresponding author: Xiaowei Li (lixwei@lzu.edu.cn)

This work was supported in part by the National Natural Science Foundation of China under Grant 61632014, Grant 61802159, Grant 61210010, and Grant 61402211, in part by the National Basic Research Program of China (973 Program) under Grant 2014CB744600, in part by the Program of Beijing Municipal Science & Technology Commission under Grant Z171100000117005, and in part by the Talent innovation and entrepreneurship project of Lanzhou (2015-RC-60).

ABSTRACT Resting-state electroencephalography (EEG) studies have shown significant group differences in functional connectivity networks between patients with depression and healthy controls. The present study aims to identify the altered EEG resting-state functional connectivity patterns of depressed patients, which can be used to test the feasibility of distinguishing individuals with depression from healthy controls. In the present study, the phase lag index was employed to construct functional connectivity matrices. An altered Kendall rank correlation coefficient was used to identify the features with high discriminative power, and several classifiers were employed to classify a total of 27 depressed patients and 28 demographically matched healthy volunteers. Permutation tests were used to evaluate classifier performance. The best classification results demonstrate that more than 92% of subjects were correctly classified by binary linear SVM through leave-one-out cross-validation for the full frequency band, and the AUC was 0.98. Our findings suggest that the depression affects brain activity in nearly the whole cortex and that changes in brain oscillation patterns in the delta, theta, and beta frequency bands are more significant than those in the alpha frequency band. The current study sheds new light on the pathological mechanism of depression and suggests that EEG resting-state functional connectivity analysis may identify potentially effective biomarkers for its clinical diagnosis.

INDEX TERMS Depression, EEG, functional connectivity, multivariate pattern analysis, resting-state.

I. INTRODUCTION

Depression is a common mental illness that already affects more than 350 million people worldwide [1], and its main characteristics are persistent, pervasive and serious depressed mood or anhedonia. The patient has difficulty controlling his mood, has a lowered mood and has decreased interest or pleasure in all activities [2]. The pathophysiology of depression remains unclear. Furthermore, it is estimated by the World Health Organization that depression will become the second leading cause of illness by 2020 [3]. Depression is the main cause of suicide, and up to 10% of people with depressive episodes will commit suicide if untreated.

The associate editor coordinating the review of this manuscript and approving it for publication was Jiachen Yang.

The human brain is a complex system comprising 100 billion (10^{11}) neuron cells and approximately 100 trillion (10^{14}) synapses [4], which are organized by dynamic neural communications and mutual interactions based on synchronous oscillations among different brain regions [5]–[7]. In recent years, a considerable body of literature has examined the synchronous oscillation patterns that reflect the activity of the brain and provide reliable markers of brain function or dysfunction [8], [9]. Therefore, it is simple and effective to explore brain activity via brain synchronous oscillatory patterns. For example, Ritz and Sejnowski [10] described intrinsically bursting pyramidal cells and discovered inhibitory interneurons that fire spike doublets to induce synchrony.

Current clinical diagnostic methods for depression have many obvious disadvantages, which include patient denial,

poor sensitivity, subjective bias and inaccuracy [11], [12]. Therefore, to exploit simple, accurate and operable methods for depression detection or to find useful biomarkers for depression is one of the most difficult challenges [12], [13]. At present, many imaging technologies are used to explore and treat mental illness, such as epilepsy and depression, including electroencephalography (EEG), functional magnetic resonance imaging (fMRI), magnetoencephalogram (MEG) recording, positron emission tomography (PET), diffusion tensor imaging (DTI), and single photon emission computed tomography (SPECT). Among them, PET and SPECT require injecting radioactive substances into the subjects. EEG is a noninvasive and painless method of evaluation of brain function which is often used in the auxiliary diagnosis of illnesses such as depression, seizure, Alzheimer, and schizophrenia [14], [15]. The advantages of EEG are sensitivity, relatively low cost and convenience for recording the activity of the brain. EEG synchronous oscillations are rhythmic electrical events coming from the brain and can be used to define the interaction between different brain regions. Due to this peculiarity, it is suggested that the information processing of the brain can be reflected in EEG oscillation rhythms [16]. Based on this theory, many findings have been presented on the study of depression [17]–[19]. For example, some results demonstrated that patients with depression had different oscillations in different frequency bands, such as delta, theta, alpha [20], and beta bands [21], [22]. An EEG oscillation study on patients with depression reported that major depression affects brain activity in nearly the whole cortex and manifests itself through considerable reorganization of the composition of brain oscillations in a broad frequency range: 0.5–30 Hz [23].

In recent years, the results of research based on different approaches, such as frontal EEG asymmetry [24], different frequency bands [25], “small-world” network characteristics [26], and increased/disrupted cognition connectivity networks [27], in patients with depression have been widely presented. These research findings revealed different neurophysiological characteristics of depression [7]. These studies have also contributed many new methods for research related to depression and provided new scientific support for explaining the mechanism of depression. Nonetheless, the scientific community still does not have a consensus on the physiological mechanism of depression [2]. In view of this, new methods and techniques and larger scale experiments for exploring depression are expected.

More recently, functional connectivity was used to identify the differences between patients with and without mental illness and classify them through the distribution of those differences[28]. Because fMRI technology has better spatial resolution information than EEG, in some studies, functional connectivity was constructed by fMRI data. For example, Anderson et al. [29] determined functional connectivity by fMRI and successfully distinguished patients with autism from control subjects with a total accuracy of 79% by a leave-one-out classifier. Liu et al. [30] classified patients with social

anxiety disorder from healthy controls using linear SVM and whole brain functional connectivity, and the results showed an 82.5% correct classification rate.

Furthermore, there are many studies using kinds of classification techniques and feature extraction methods based on EEG signals and functional connectivity networks constructed by EEG signals to discriminate between depressed patients and normal controls. For instance, Erguzel et al. [31] optimized a classification by a combinative genetic algorithm and a back-propagation neural network for classifying major depressive disorder (MDD) and normal patients, and the outcomes of his approach indicate the noticeably increased overall accuracy of 89.12%. In the paper [32], a classification accuracy of 90% is achieved by all nonlinear features and a logistic regression classifier. Mumtaz et al. [33] proposed a machine learning framework with synchronization likelihood features to discriminate MDD patients and normal controls; the most successful results indicated that the classification accuracy was 98% using an SVM classifier from 34 MDD patients and 30 healthy subjects. As a data-driven technique, multivariate pattern analysis based on whole brain EEG functional connection can complement univariate statistical analyses. In recent years, there has been increasing interest in multivariate pattern analysis methods to investigate changes in the brain using brain activity data from fMRI, EEG, MEG and other brain imaging techniques [34]–[36].

In addition, several previous studies using EEG have demonstrated that depression can affect the activity of the resting state of the brain. Relevant researchers have indicated the use of the resting-state for recognizing mild depression [37]–[40]. However, to date, it is unknown whether multivariate pattern analysis can capture whole brain EEG resting functional connectivity patterns to discriminate depressed patients from normal controls at the individual subject level with a high degree of accuracy.

The purpose of this study was to explore significantly altered EEG functional connectivity patterns and to discriminate patients with depression from healthy subjects. Altered EEG functional connections were expected to be observed in resting state networks. Therefore, in this study, we adopted a resting-state paradigm to collect EEG and discriminate between patients with depression and normal controls. The sensory data from EGI (electrical geodesics, Inc., USA) 128 channel devices were preprocessed with MATLAB programs. In cleaned EEG data, we constructed phase lag index (PLI) matrices for each subject. Then, the high discriminative power features were extracted by the altered Kendall rank correlation coefficient for several familiar classifiers, including support vector machine (SVM) [41], decision tree (DT), k-nearest neighbor (KNN) and naïve Bayes (NB) classifiers. To test the generalization ability of the classifier, we performed a permutation test on the SVM classification’s results. This study will be helpful in further understanding the neural mechanisms underlying the behavioral symptoms of depression, which may offer additional information for

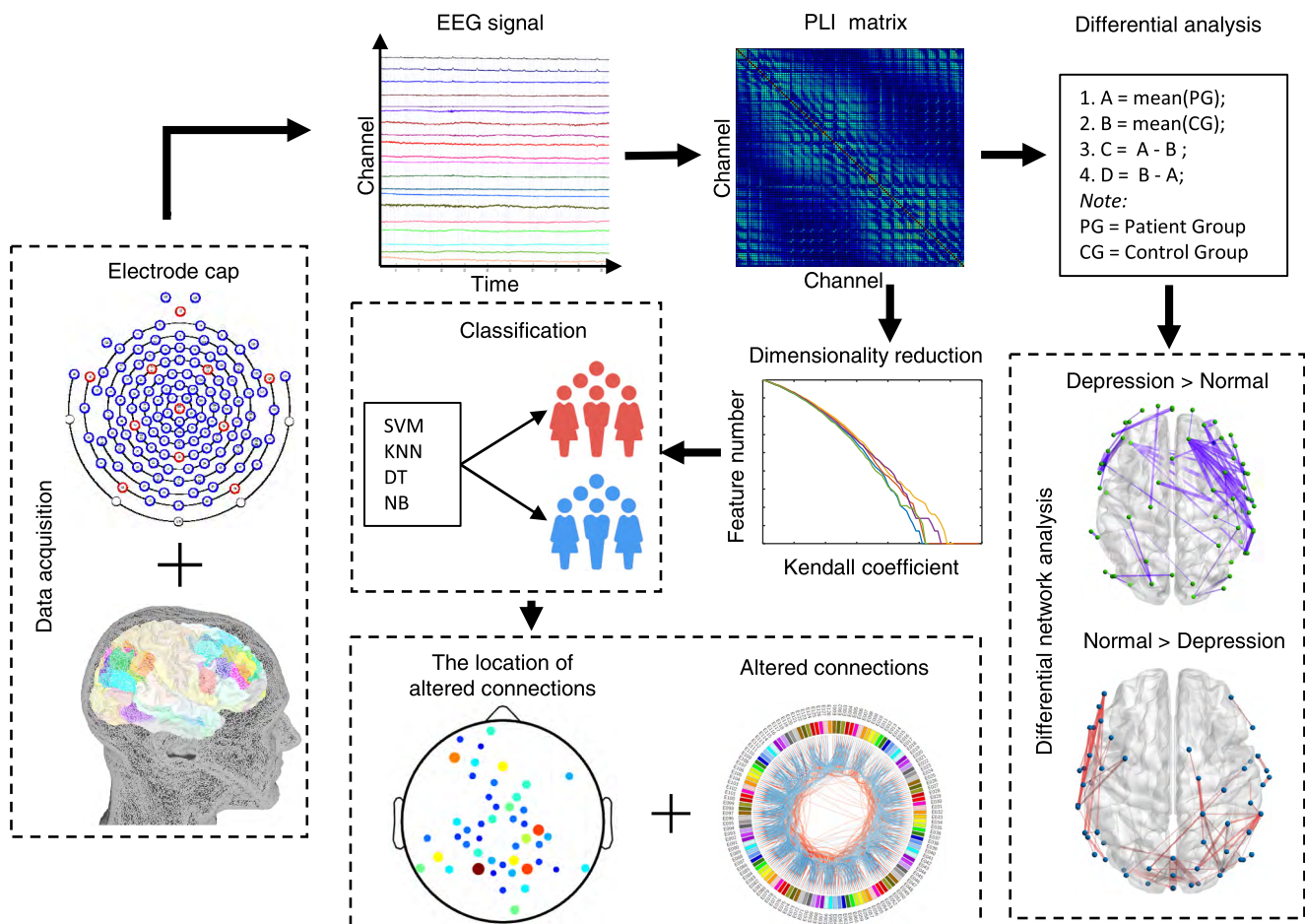


FIGURE 1. Flowchart for functional connectivity and multivariate pattern analysis.

advancing our understanding of the pathophysiology of the disorder.

II. MATERIALS AND METHODS

The proposed procedure for the analysis of functional connectivity and multivariate pattern analysis for depression identification is summarized in Figure. 1.

A. SUBJECTS

Written informed consent was obtained before the experiment began. The participants included 30 patients diagnosed with MDD from the clinic at Lanzhou University Second Hospital of China (Lanzhou, Gansu Province of China), and 30 similar normal volunteers were recruited from the community. All of the subjects were native Chinese speakers. MDD patients were chosen according to their score on the PHQ-9 [42] and GAD-7 [43], and confirmation of the diagnosis was made by clinical psychiatrists. Exclusion criteria included any kind of neurological disorder, serious head injury with loss of consciousness, acute physical illness and presence of drug or alcohol abuse. Similar exclusion criteria were adopted for healthy control subjects. To ensure the effectiveness of this study, the exclusion criteria were strictly enforced before

TABLE 1. Characteristics of the participants in this study.

Characteristic	Mean \pm SD		p-value
	Patient	Control	
Number	27	28	
Gender (Female/male)	11F/16M	9F/19M	0.51 ^(a)
Age(years)	31.67 \pm 10.94	31.82 \pm 8.76	0.95 ^(b)
Score of PHQ-9	17.89 \pm 3.56	2.75 \pm 1.84	0.00 ^(b)
Score of GAD-7	13.52 \pm 4.93	1.93 \pm 1.89	0.00 ^(b)

^a Chi-square test.

^b Two-sample t-test.

the experiment. Three patients and two normal volunteers' data were rejected from the sample due to the lack of some basic information or to too much noise during EEG acquisition. Finally, 27 MDD and 28 healthy sex- and age-matched subjects remained. Detailed statistical information is summarized in Table 1.

B. DATA ACQUISITION AND PREPROCESSING

The resting state EEG data were recorded by the 128-channel HydroCel Geodesic Sensor Net and Net Station software at

a sampling rate of 250 Hz and referenced to the vertex (Cz electrode), and electrode impedances were kept below 70 k Ω . In the experiments, participants sat in a dimly lit and quiet room and were asked to remain still with their eyes closed for 5 minutes. Then, the subjects were instructed to be comfortably seated on a wooden chair, keep their eyes closed, relax, remain awake and to perform no specific cognitive exercise during the EEG recording. Simultaneously, they were also required to reduce head and body movement and eye movement to achieve a reduction in electromyography (EMG) and electrooculography (EOG) noise, respectively [44].

The resting state EEG data were further processed offline with the MATLAB EEGLAB¹ toolbox and several plugins. First, the EEG data were filtered (bandpass = 1–40 Hz) using a Hamming windowed Sinc FIR filter [45]. Electrical interference from the 50 Hz-line noise and the “baseline drift” were removed by this filter. Second, the EEG data were manually inspected, and nonbrain-related artifacts such as muscle contractions and movement-related artifacts, also called EMG, and eye movements (EOG, electrooculography), were removed by the TrimOutlier plugin.² In this step, bad channels and bad data points were repeatedly rejected by threshold-set reference mean and SD values. Third, the location of removed bad channels was interpolated using spherical interpolation. The interpolation method can complete the recording of EEG, but this causes a rank deficiency. Fourth, from the historical research, the use of the REST [46] re-referencing approach is better than the average re-referencing approach. Therefore, the REST re-reference was applied to all of the EEGs. Fifth, after the above steps, the remaining data points included some high-power content, and some EEG epochs were removed by Artifact Subspace Reconstruction (ASR) plugin.³

Through the above steps, cleaned EEG data were produced. For a better understanding of human brain activity, the EEG signal waves were divided into four major sub-bands, which were divided from low to high frequencies known as delta (δ , range 1–4 Hz), theta (θ , range 4–8 Hz), alpha (α , 8–13 Hz), and beta (β , 13–30 Hz) bands. The present study investigated the whole frequency EEG band and four EEG sub-band signals.

C. PHASE LAG INDEX ANALYSIS AND CONSTRUCTION OF THE FUNCTIONAL CONNECTIVITY MATRIX

Researchers have explored some methods of functional connectivity for quantifying phase synchronization in multichannel EEG, such as phase coherence (PC) [47] and imaginary component of coherency (IC) [48] analysis. The PLI (Phase Lag Index) [49] is used to obtain reliable estimates of phase synchronization that are invariant against the presence of common noise sources. With two given EEG signals x and y considered, the PLI value is calculated by the following

equations, where $k = 1 \dots N$.

$$PLI_{xy} = |\langle \text{sign}[\theta_x(t_k) - \theta_y(t_k)] \rangle| \quad (1)$$

The PLI value ranges between 0 and 1: $0 \leq PLI \leq 1$, where 0 indicates either no coupling or coupling with a phase difference centered around $0 \bmod \pi$, and 1 indicates completed phase locking at a value of $\Delta\theta(t_k) = \theta_x(t_k) - \theta_y(t_k)$ different from $0 \bmod \pi$. In equation (1), $|x|$ denotes the absolute value of X , and $\langle \cdot \rangle$ denotes the mean of Y vector. Where $\text{sign}()$ is a signum function, the result of $\text{sign}[Z_1 - Z_2]$ denotes positive or negative 1; if $Z_1 > Z_2$, the value is 1, otherwise, the value is 0.

$$\theta_x(t_k) = \arctan \frac{\tilde{x}(t_k)}{x(t_k)} \quad (2)$$

$$z(t_k) = x(t_k) + i\tilde{x}(t_k) = A(t_k) e^{i\theta(t_k)} \quad (3)$$

In (1), $\theta(t_k)$ denotes the instantaneous phase of the signal, which can be computed by (2). The analytical signal $z(t_k)$ is a complex-value, $x(t_k)$ a real-time series and $\tilde{x}(t_k)$ its corresponding Hilbert transform.

Through the above computational equations, we evaluated functional connectivity between each pair of channels using PLI_{xy} . Thus, for each subject, we obtained a resting-state functional connectivity captured by a 128×128 symmetric matrices C_{ij} :

$$C_{ij} = \begin{bmatrix} C_{11} & C_{12} & \dots & C_{1n} \\ C_{21} & C_{22} & & C_{2n} \\ \vdots & & \ddots & \vdots \\ C_{n1} & C_{n2} & \dots & C_{nn} \end{bmatrix}_{128 \times 128} \quad (4)$$

In this matrix, each row and column corresponds to a different node, and the matrix element positioned at the intersection of the i th and j th columns encodes information about the connection between channels i and j . In this study, the subscripts of C were used to index each element, the first subscript i indexes rows and the second subscript j indexes columns. Diagonal elements C_{ij} (where $i = j$) of the connectivity matrix with the black font in equation (4) are set to 1, and off-diagonal elements C_{ij} (where $i \neq j$) with red and blue font are set to PLI_{xy} value.

D. ALTERED KENDALL RANK CORRELATION COEFFICIENT AND FEATURE DIMENSION REDUCTION

For each symmetric functional connectivity matrix, 128 diagonal elements were removed, and the upper triangle elements of the connectivity matrix were extracted as classification features, i.e., the feature space for classification was constituted by the $128 \times (128 - 1)/2 = 8128$ dimensional feature vectors.

The abnormal functional connectivity patterns associated with depression are mainly represented by the highly discriminating functional connections, and 8128-dimensional feature vectors including all the differences caused by lesion and noise. Highly discriminatory features were selected from the original 8128 features space, further reducing the number of features, accelerating computation and diminishing

¹EEGLAB Wiki: <https://sccn.ucsd.edu/wiki/EEGLAB>

²TrimOutlier plugin: <https://sccn.ucsd.edu/wiki/TrimOutlier>

³Clean_rawdata (ASR): <http://sccn.ucsd.edu/eeqlab/plugins/ASR.pdf>

noise [50]. Therefore, the feature selection method was used to reduce the dimension for classification through retaining the most discriminative functional connections and eliminating the remaining indistinctive features. The discriminative power of a feature can be quantitatively measured by the importance of its degree of relevance to classification. We adopt a kind of altered Kendall rank correlation coefficient, commonly referred to as the Kendall's tau coefficient [51], to measure the correlation of each connection with the classification, which provides a distribution-free test of independence between two variables.

If there are m subjects in the patient group and n subjects in the normal control group, X_{ij} denotes the i th functional connectivity feature of the j th subject, and Y_j denotes the class label of a particular sample (+1 denotes a patient subject and -1 denotes a normal control subject), the altered Kendall rank correlation coefficient τ_i of the functional connectivity feature can be defined as:

$$\tau_i = \frac{n_c - n_d}{m \times n} \quad (5)$$

where n_c is the number of concordant pairs and n_d is the number of discordant pairs. Because the relationship between a pair of subjects that belong to the same group is not considered, the total number of subject pairs is $m \times n$. For a pair of two-observation data sets $\{X_{ij}, Y_j\}$ and $\{X_{ik}, Y_k\}$, a concordant pair is when

$$\text{sign}(X_{ij} - X_{ik}) = \text{sign}(Y_i - Y_k) \quad (6)$$

Correspondingly, a discordant pair is when

$$\text{sign}(X_{ij} - X_{ik}) = -\text{sign}(Y_i - Y_k) \quad (7)$$

From the above method, for τ_i , a positive value indicates that the i th functional connectivity increased in the patient group compared to the normal control group, and a negative value indicates that the i th functional connectivity decreased in the patient group compared to the control group. The discriminative power of a feature was defined as the absolute value of the Kendall correlation coefficient $|\tau_i|$. Then, the features were ranked according to their discriminative power from large to small, and a set of coefficients over a specified threshold was selected as the final feature space for classification.

E. CLASSIFICATION AND PERFORMANCE EVALUATION

When the dataset of features with high discriminative power was obtained, binary support vector machine (SVM) with a linear kernel function and a k-nearest neighbor (KNN) with 1 neighbor, decision tree (DT) and naïve Bayes (NB) classifiers were employed to solve the classification problem. The results were reported with the default parameter setting. For the support vector machine classifier, we adopted the LIBSVM [41] program package, and the SVM type was C-SVC. For the other classifiers, the main analysis programs are from the Statistics and Machine Learning Toolbox in MATLAB. Due to the limited number of samples, we used

a leave-one-out cross-validation strategy to estimate the generalization ability of our classifier. In the current study, the performance measure of a classifier is quantified using the sensitivity (true positive rate), specificity (false positive rate), accuracy, receiver operating characteristic (ROC) curve and area under the ROC curve (AUC) based on the result of cross-validation. Note that the sensitivity represents the proportion of patients correctly predicted, and the specificity represents the proportion of normal controls correctly predicted.

F. STATISTICAL INFERENCE WITH PERMUTATION TESTS

Many frameworks for statistical tests for assessing classification performance have been explored by researchers [52], [53]. In this study, we chose the AUC as the statistic to test the generalization ability GR of the classifier. Permutation tests were employed to estimate the statistical significance of the observed classification generalization ability. In permutation testing, the class labels of the training data were randomly permuted prior to training. Then, cross-validation was performed on the permuted training set, and the permutation was repeated 10000 times. Suppose that a classifier learned reliably from the data when the generalization ability GA_0 obtained by the classifier trained on the real class labels exceeded the 95% confidence interval of the classifier trained on randomly relabeled class labels. For any value of the estimated GA_0 , the appropriate P -value $\hat{P}(GA_0)$ represented the probability of observing a classification prediction rate no less than GA_0 . Then, the null hypothesis was rejected because those classifiers could learn the relationship between the data and the labels reliably and declare that the classifier learned the relationship with a probability of being wrong of at most $\hat{P}(GA_0)$.

III. RESULTS AND DISCUSSION

A. FUNCTIONAL CONNECTIVITY MATRIX AND LOCATION DISTRIBUTION

The number of connections between these channels is large; for any network of N nodes, the number of possible connections is in the order of N^2 . Thus, we used a connectivity matrix to represent the large dataset in a simple and meaningful way. The connectivity matrix offers a compact description of the pairwise connectivity between all nodes of a network as a two-dimensional matrix. A PLI functional connectivity matrix was calculated for each subject between all of the electrodes on the scalp. As shown in Figure 2, the PLI functional connectivity matrices of both groups show complex but similar patterns with various regions of high (redder) and low (bluer) levels of synchronization. However, there was no evident difference in the distribution of highlighted areas between the groups. From the difference matrix (Figure. 2c) and compared with the normal control group, the patient group with depression exhibited an increased degree of synchronization in a small area, but in a large area, the patient group exhibited a reduced degree of synchronization from the difference matrix (Figure. 2d). In general, there are fewer

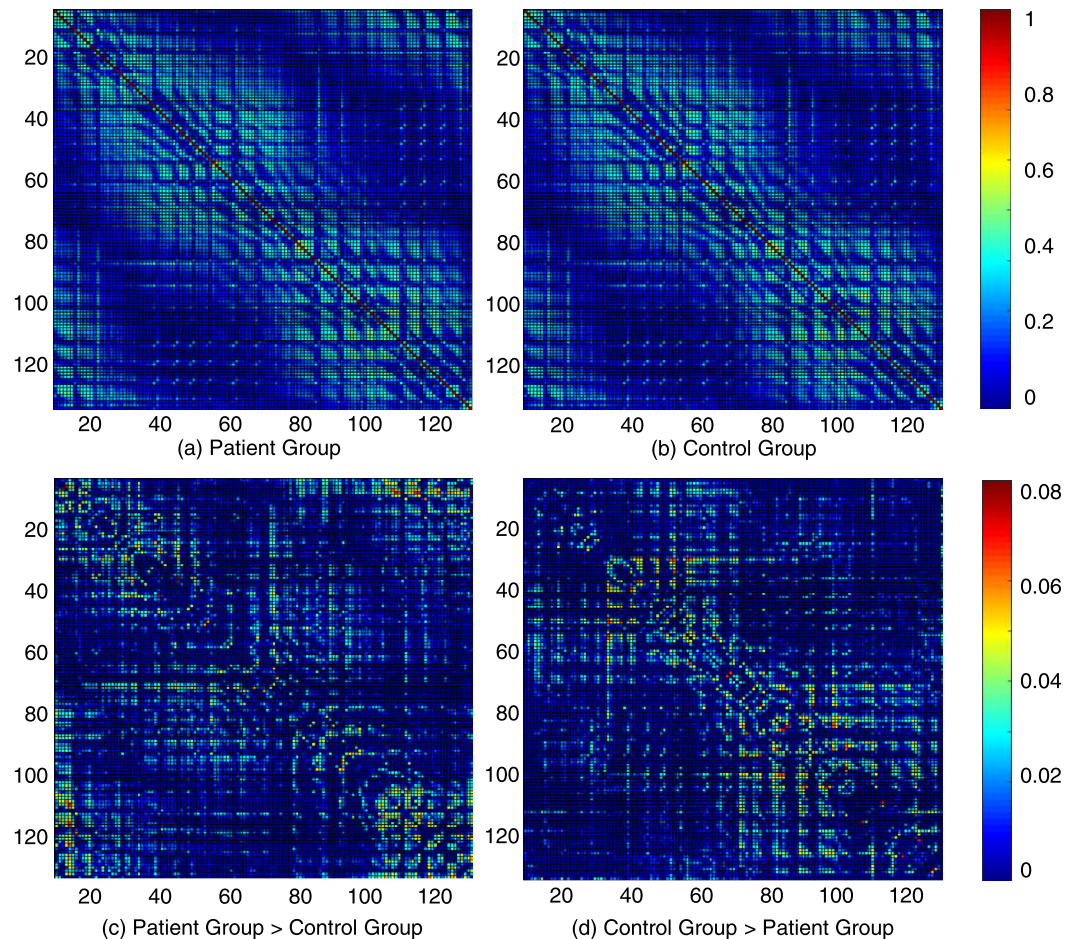


FIGURE 2. Weighed phase lag index functional connectivity network measured with the whole frequency band EEG. (a) Mean functional connectivity matrices for the depressive patient group ($N = 27$). (b) Mean functional connectivity for normal control subject group ($N = 28$). (c) and (d) indicates the difference matrix of patient group and normal control group, (c) Patient group > Control group, (d) Control group < Patient group. In the matrix map, the horizontal and vertical axes denoted 128 channels, and each chromatic point represented the PLI value of two corresponding channels. Note, other bands information is in the Appendix.

connections for the patient group than the normal control group, but the strength is large. There are more connections in the normal control group than in the patient group, but the strength is smaller.

To explore the location distribution of the difference matrix of the scalp, we plotted the difference matrix in a 3D graph according to the location of the channels, as shown in Figure 3. For the full frequency band, with a threshold of 0.05, most of the areas with increased connection density were distributed in the left frontal, temporal, and parietal lobes and in the right occipital lobe. Most of the areas with decreased connection densities were distributed in the right frontal lobe. In the delta band, we found that increased connection densities were mainly located in the left temporal lobe, and decreased connection densities were spread across the whole brain. From a physiological point of view, delta frequency waves mainly appear in the adult sleeping state and are spread widely [2]. In the theta band, most of the areas of increased connection density were distributed in the right occipital lobe, and most of the areas with decreased connection density were

distributed in the left frontal lobe. In the alpha band, most of the areas with increased connection density were distributed in the left frontal lobe, and most of the areas with decreased connection density were distributed in the left parietal lobe. In the beta band, most of the areas with increased connection density were distributed in the left parietal lobe, and most of the areas with decreased connection density were distributed in the left frontal and temporal lobe. Most of the previous literature has revealed an increase in functional connectivity in different frequency bands for patients with depression in the resting state. For example, Leuchter et al. examined resting-state functional connectivity in different frequency bands and found that MDD subjects expressed higher theta and alpha coherence in longer distance connections between frontopolar and temporal or parietooccipital regions and higher beta coherence primarily in the dorsolateral prefrontal cortical or temporal regions [38]. Many fMRI studies have found that brain networks have increased connectivity in different brain regions in depression patients [54]–[56]. Similarly, for EEG research, several studies have reported that there was

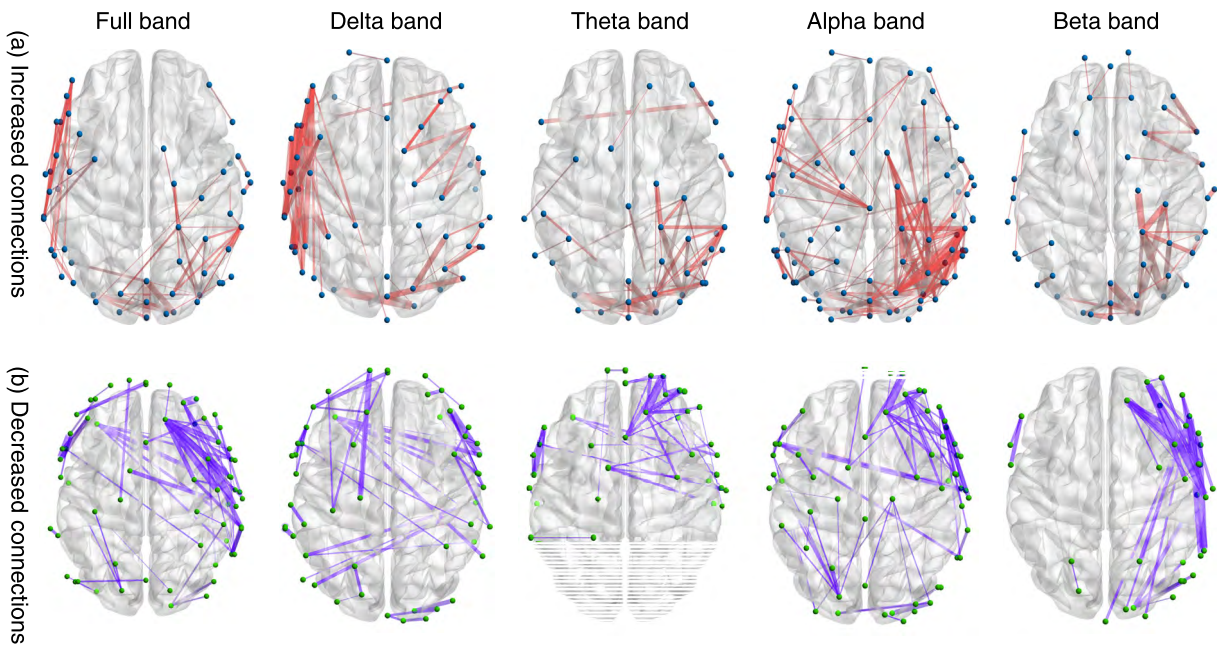


FIGURE 3. The location distribution of the difference matrix in five frequency bands. (a) the increased connections for patients with depressive. (b) the decreased connections for the patient.

an abnormal power spectrum, asymmetry, and coherence in some frequencies [57]. However, some studies also discovered decreased brain functional connections [58], [59]. Many improvements have been made, but due to the use of different methods and data, there are differing results. We hypothesize that the EEG synchronization pattern of the entire brain has changed in each band, but the degree of change is different. In the future, more research is needed to explore the relevant changes. The results of the PLI functional connectivity analysis and the location distribution showed that the patients with depression had significantly higher synchronization in the left hemisphere of the brain, especially in the frontal, temporal and parietal lobes and in the occipital lobe of the right hemisphere, and lower synchronization in the right hemisphere of the brain, especially in the frontal lobe, compared with the normal control group in the full wave band.

B. CLASSIFICATION RESULTS

Because different classifiers yield different results for the same feature set, we used a different feature set for the different classifiers. In this study, we used 4 kinds of classifiers and recorded the best result for each classifier. Because the main purpose of this study is to explore the altered connections in different frequency bands and brain regions of patients with depression, these classification methods were also applied to the delta, theta, alpha, and full bands. We recorded each result of the different classifiers and different frequency bands using leave-one-out cross-validation. The performance results are shown in Table 2. Table 2 shows that the binary linear support vector machine classifier achieved an accuracy of 92.73% (area under the ROC curve is 0.98, < 0.0001) in the full frequency wave band. For each individual frequency band, the best classification is also SVM; in addition, the

classification accuracies of the full, delta and theta bands are better than the alpha and beta bands. Therefore, we suggest that there exists a significant between-group difference in the full, delta and theta bands that could be used for classification. From Table 2, we can see that the decision tree and naive Bayes classifiers yielded the same classification accuracies and ROCs as seen in Figure 4b.

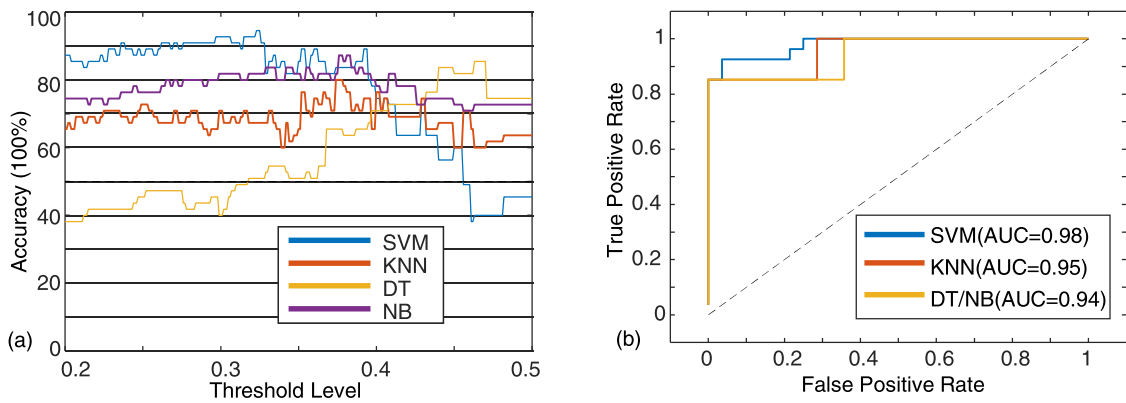
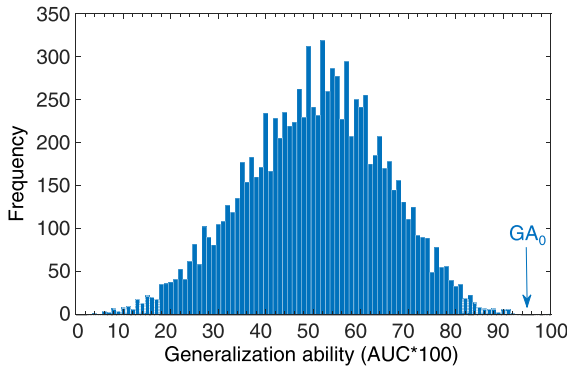
Previous studies have indicated significant differences between depression patients and normal controls in the theta band [7] and alpha band [7], [60]. However, there is not a definitive result, and there are still many controversies. In this study, our results show that depression patients and normal subjects can be distinguished by the variation of functional connections at different frequency bands. This change not only occurs in the alpha and theta bands but also in the entire frequency band. Because different thresholds will lead to different numbers of features, there are different results with a different threshold level for the same classifier, and the accuracy of the four classification methods based on different thresholds is shown in Figure 4a.

From Table 2, the SVM classifier achieves the best classification results for the entire frequency band of EEGs, and overfitting did not occur. For other classifiers, the default parameters are used. For the same feature space, the classification effect is not as successful as the SVM classifier. Due to the variation in sensitivity to the number of features for each classifier, performance differences cannot be avoided.

From the classification results, we found that the SVM approach is the best classification method for different frequency bands. To verify the correctness and generalization ability of the SVM classifier, we performed a permutation test with the AUC as the test statistic, and the permutation was repeated 10000 times. The permutation distribution of

TABLE 2. classification results of four classifiers on the different frequency band.

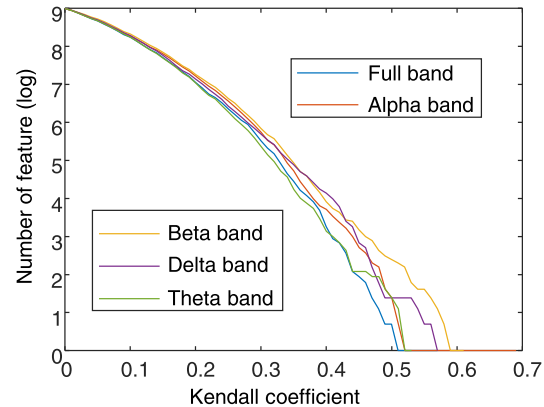
Classifier	SVM		KNN		DT		NB	
	accuracy	features number						
full (1-40Hz)	92.73%	249	78.18%	50	85.46%	4	85.46%	50
delta (1-4Hz)	90.91%	255	80.00%	26	74.55%	9	83.64%	9
theta (4-8Hz)	90.91%	268	85.46%	55	72.73%	20	87.27%	215
alpha (8-13Hz)	80.00%	606	76.36%	15	72.73%	606	78.18%	25
beta (13-30Hz)	87.27%	882	78.18%	20	81.82%	24	83.64%	20

**FIGURE 4.** (a) The changes in the accuracies of four classifiers as a function of threshold and (b) ROC curves of depression patients for four classifiers based on functional connectivity.**FIGURE 5.** The permutation distribution of the estimate using the binary linear support vector machine classifier (repetition times = 10000) when retaining the 249 most discriminating power features: x and y labels represent the generalization ability ($AUC \times 100$) and frequency, respectively. G_A_0 is the generalization ability obtained by the classifier trained on the real class labels.

the estimate is shown in Figure 5, indicating that the SVM classifier learned the relationship between the data and the labels with a probability of being wrong of < 0.0001 .

C. ALTERED FUNCTIONAL CONNECTIVITY

Informed by the above classification results, we extracted features with high discriminative power from each connection. The discriminative power of each connection was quantified by the altered Kendall rank correlation coefficient for classification. To choose the best threshold to achieve the best classification effect, we performed statistics on the number of features under different thresholds, as shown in Figure 6. In one extreme case (threshold < 0.2), all connections were

**FIGURE 6.** The distribution of the characteristics of different frequency band data as a function of the altered Kendall rank correlation coefficient.

considered major features for classification. In the other extreme case (threshold > 0.5), there were only a few connections selected as features. In these cases, most of the classifiers did not perform well. In different frequency bands, the discriminative power of the number of features had a trend similar to the threshold changes. Since we used a leave-one-out cross-validation strategy to estimate the generalization ability of the classifiers (see below) and feature ranking is based on a slightly different training dataset in each iteration of the cross-validation, the final feature set differed slightly for each iteration. In this study, we assessed each classifier performance at the different thresholds, and we selected a distribution of discriminative power features that had the best classification performance using a binary SVM classifier, as shown in Figure 7. The electrodes related to consensus

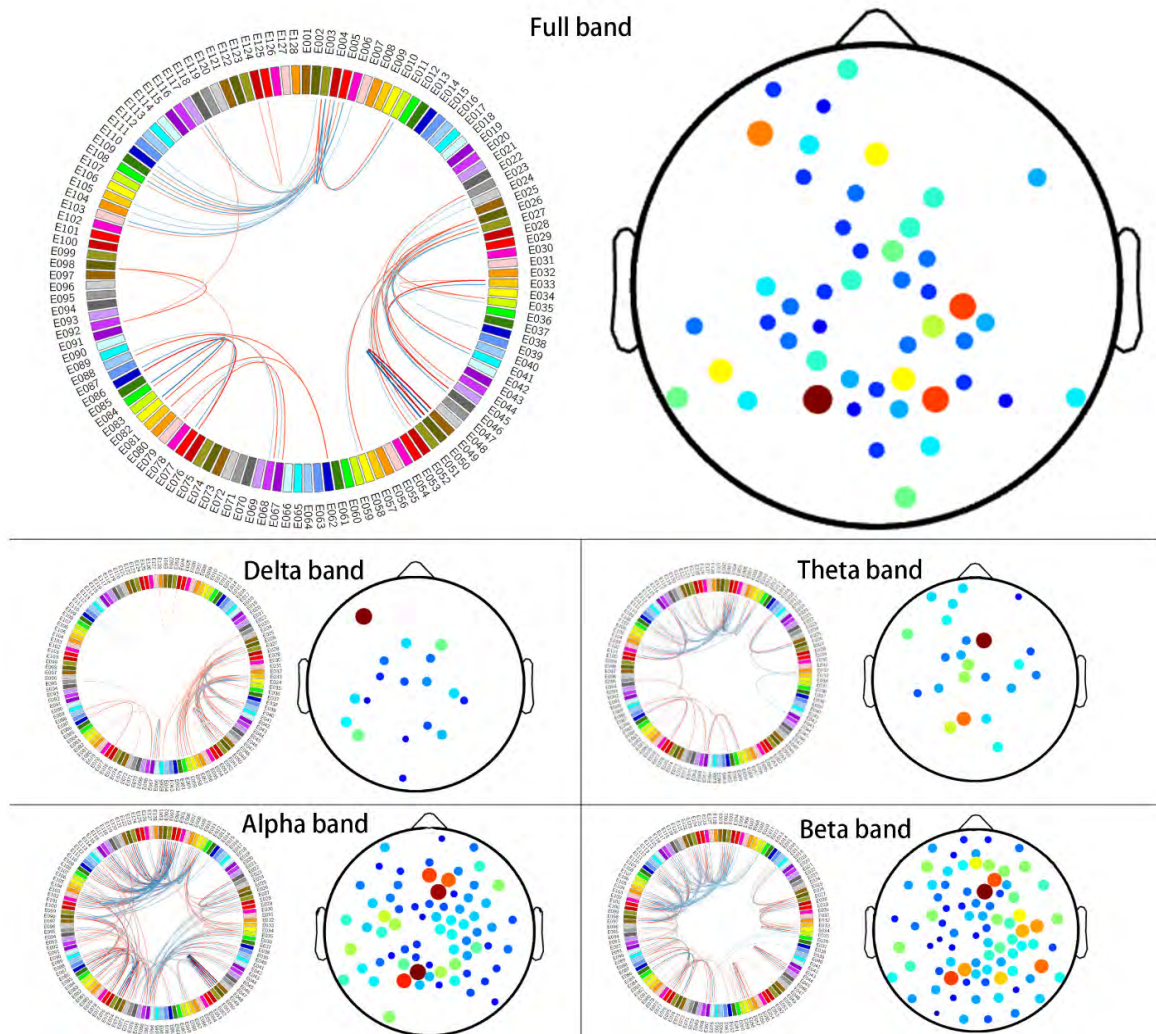


FIGURE 7. The distribution of high discriminative power of resting-state functional connectivity assessed with EEG for the patient group with depression and the normal control group. (left) A circular projection of the difference in functional connectivity in the best SVM classification performance for a different frequency. The red edges linking different channels indicate consensus connections from patients with depression, and the blue edges indicate consensus connections from the normal control group. (right) The location of electrodes with high discriminative connections; the size of a node indicates the degree fraction of node. The color of nodes does not represent any characteristic.

functional connectivity for patients with depression are primarily located in the left frontal lobe and parietal lobe in the whole frequency band, as shown in Figure 7. Therefore, our results suggest that functional connectivity between the left frontal lobe and parietal lobe was altered in depressed patients as well. For the delta and theta frequency band, we found that the number of important nodes was smaller and the distribution was sparser than those of the other bands. For high-frequency bands such as alpha and beta bands, the number of important nodes was more densely distributed.

In a previous study, Zeng et al. [61] attempted to distinguish depressed patients from healthy controls using machine learning methods and fMRI data, and they not only achieved an individual-level classification consistency of 92.5% but also revealed that the subgenual cingulate functional connectivity network may play a critical role in patients with depression. In this study, we found that this machine learning

approach can be used not only for fMRI data through computational analysis but also for the analysis of functional connectivity based on EEG.

With respect to theta activity, previous studies suggested that altered theta activity may explain disrupted functional connectivity in frontal-cingulate pathways mediating emotive regulation in patients with depression [62], [63]. Because this study is limited to the scalp over the brain, the location of altered theta oscillation patterns could not be observed. For the alpha oscillations, the number and strength of the short-range anterior and posterior functional connections were proportional to MDD severity [60]. Based on the current findings, we suggest that global short-range functional connections within alpha and beta oscillations seem to play an important role in the pathogenesis of MDD and its severity. Fingelkurts et al. [23] found that major depression affects brain activity in nearly the whole cortex and manifests itself

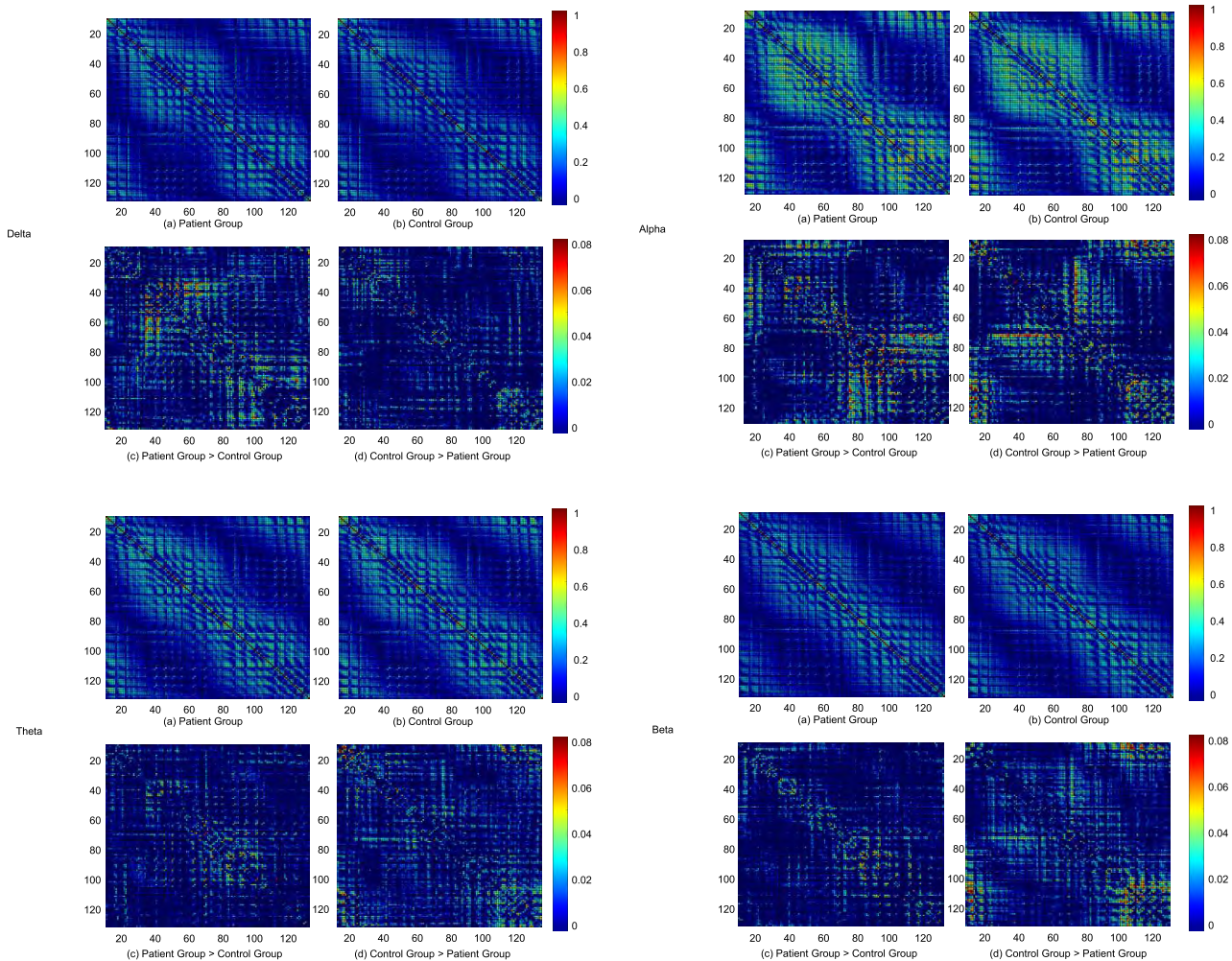


FIGURE 8. Weighed phase lag index functional connectivity network measured with the Delta, Theta, Alpha and Beta frequency bands EEG.
(a) Mean functional connectivity matrices for the depressive patient group ($N = 27$). **(b)** Mean functional connectivity for normal control subject group ($N = 28$). **(c)** and **(d)** indicates the difference matrix of patient group and normal control group, **(c)** Patient group > Control group, **(d)** Control group < Patient group. In the matrix map, the horizontal and vertical axes denoted 128 channels, and each chromatic point represented the PLI value of two corresponding channels.

as a considerable reorganization of the composition of brain oscillations in a broad frequency range (0.5-30 Hz) and that the magnitude of the effect of depression was maximal in the left anterior and posterior cortex of the brain. From the results of the current study, we assert that depression affects brain activity in nearly the whole cortex, and in the low-frequency EEG bands such as delta and theta, the difference is mainly manifested in the occipital region and the left prefrontal lobe. This has more overlap with the brain regions involved in the current default mode network in the fMRI field. At the same time, this difference distribution also shows the prefrontal asymmetry, the difference is mainly located in the left prefrontal.

IV. CONCLUSIONS AND FUTURE WORK

In conclusion, in this study collected and analyzed EEG data for the resting state of 55 subjects. To provide a more efficient method for detecting mildly depressed patients, we employed an altered Kendall ranked correlation coefficient and four classification algorithms. It was found that the binary linear

SVM classifier had best performance and that compared to the sub-band, the full band was abnormally changed, with a classification accuracy above 92% and an AUC above 0.98. The combination of a linear SVM and the full frequency band was considered to be more efficient, more accurate and more robust to discriminate patients with depression and normal controls. We also analyzed the discriminative feature set distribution across the brain regions, and the results indicated that the left hemisphere and right hemisphere have many differences, especially the left frontal and whole parietal lobes. Finally, we suggest that depression affects EEG resting-state brain activity in a broad frequency range (1-40 Hz) rather than in only the theta band or in the other frequency bands. At the same time, the degree of the effect of depression was maximal in the left anterior and posterior cortex of the brain.

The spatial distribution of differences from functional connectivity matrices and of high discriminative power connections is not exactly the same. This discrepancy may be caused by the different analysis methods. However, the distribution differences caused by the PLI functional connectivity

TABLE 3. The parameter settings of classifiers, the default parameter settings were used as the table in the article.

The parameter settings of classifiers, the default parameter settings were used as the table in the article.

Classifier	Command and Parameters
SVM	Command: <code>svmtrain(labels,traindata,'-s 0 -t 0 -v 55 -q');</code>
KNN	Command: <code>fitcknn(traindata,labels,'KFold',55);</code>
DT	Command: <code>fitctree(traindata,labels,'KFold',55);</code>
NB	Command: <code>fitcnb(traindata,labels,'KFold',55);</code>

matrices did not show statistically significant differences. Additionally, the identification of discriminative features by the altered Kendall rank correlation coefficient provides a new solution for examining the different characteristics of the EEG functional network. Although the classification results of this study using resting-state PLI functional connectivity are encouraging, there are still limitations related to the sample size, which was relatively small, and the lack of a large independent dataset to test our methods and confirm the findings. To continue our research, in the future, we will recruit more subjects to improve the validity of the results and to classify a range depressed states, such as mild depression. The aim of functional neuroimaging is to understand the functional organization of the brain, such as the location of processing areas, the time course or dynamics of their activities, and the nature of their interactions. Moreover, this study is only effective on the scalp, and it lacks more spatial information. In the future, we will investigate the EEG source location on the scalp (also called the inverse problem) and try to use source localization technology [64], [65] to study the changes in the brain of a patient with depression. It is hoped that these findings and methods may have the generalizability to provide an effective approach for the auxiliary diagnosis of depression and to help depressed patients take precautions early.

APPENDIX

See Figure. 8 and Table 3.

REFERENCES

- [1] K. Smith, "Mental health: A world of depression," *Nature*, vol. 515, no. 7526, p. 180, Nov. 2014.
- [2] M. Baer, B. W. Connors, and M. A. Paradiso, *Neuroscience: Exploring the Brain*. Philadelphia, PA, USA: Lippincot, Williams and Wilkins, 2007.
- [3] C. J. Murray and A. D. Lopez, "Evidence-based health policy—lessons from the global burden of disease study," *Science*, vol. 274, no. 5288, pp. 740–743, Nov. 1996.
- [4] A. Fornito, A. Zalesky, and E. Bullmore, *Fundamentals of Brain Network Analysis*. New York, NY, USA: Academic, 2016.
- [5] O. Sporns, "The human connectome: A complex network," *Ann. New York Acad. Sci.*, vol. 1224, no. 1, pp. 109–125, Apr. 2011.
- [6] B. Güntekin and E. Başar, "A review of brain oscillations in perception of faces and emotional pictures," *Neuropsychologia*, vol. 58, no. 1, pp. 33–51, May 2014.
- [7] X. Li, Z. Jing, B. Hu, J. Zhu, N. Zhong, M. Li, Z. Ding, J. Yang, L. Zhang, L. Feng, and D. Majoe, "A resting-state brain functional network study in MDD based on minimum spanning tree analysis and the hierarchical clustering," *Complexity*, vol. 2017, Jun. 2017, Art. no. 9514369.
- [8] R. W. Thatcher and J. F. Lubar, "History of the scientific standards of QEEG normative databases," in *Introduction to Quantitative EEG and Neurofeedback: Advanced Theory and Applications*, T. Budzinski, H. Budzinski, J. Evans, and A. Abarbanel, Eds. San Diego, CA, USA: Academic Press, 2008.
- [9] J. R. Hughes and E. R. John, "Conventional and quantitative electroencephalography in psychiatry," *J. Neuropsychiatry Clin. Neurosci.*, vol. 11, pp. 190–208, May 1999.
- [10] R. Ritz and T. J. Sejnowski, "Synchronous oscillatory activity in sensory systems: New vistas on mechanisms," *Current Opinion Neurobiol.*, vol. 7, no. 4, pp. 536–546, Aug. 1997.
- [11] M. Sung, C. Marci, and A. Pentland, "Objective physiological and behavioral measures for identifying and tracking depression state in clinically depressed patients," MIT Media Lab, Cambridge, MA, USA, Tech. Rep. 595, 2005.
- [12] X. Li, B. Hu, S. Sun, and H. Cai, "EEG-based mild depressive detection using feature selection methods and classifiers," *Comput. Methods Programs Biomed.*, vol. 136, pp. 61–151, Nov. 2016.
- [13] H. Cai, J. Han Y. Chen, X. Sha, Z. Wang, B. Hu, J. Yang, L. Feng, Z. Ding, Y. Chen, and J. Gutknecht, "A pervasive approach to EEG-based depression detection," *Complexity*, vol. 2018, Jan. 2018, Art. no. 5238028.
- [14] P. Giannakopoulos, P. Missonnier, G. Gold, and A. Michon, "Electrophysiological markers of rapid cognitive decline in mild cognitive impairment," in *Dementia in Clinical Practice*, vol. 24. Basel, Switzerland: Karger, 2009, pp. 39–46.
- [15] W. Zheng, Z. Yao, Y. Xie, J. Fan, and B. Hu, "Identification of alzheimer's disease and mild cognitive impairment using networks constructed based on multiple morphological brain features," *Biol. Psychiatry, Cognit. Neurosci. Neuroimag.*, vol. 3, no. 10, pp. 887–897, Oct. 2018.
- [16] F. L. Da Silva, "The generation of electric and magnetic signals of the brain by local networks," in *Comprehensive Human Physiology*. Berlin, Germany: Springer, 1996, pp. 509–531.
- [17] C. J. Stam, J. Pijn, P. Suffczynski, and F. L. Da Silva, "Dynamics of the human alpha rhythm: Evidence for non-linearity?" *Clin. Neurophysiol.*, vol. 110, no. 10, pp. 1801–1813, Oct. 1999.
- [18] C. J. Stam, "Brain dynamics in theta and alpha frequency bands and working memory performance in humans," *Neurosci. Lett.*, vol. 286, no. 2, pp. 115–118, Jun. 2000.
- [19] A. A. Fingelkurts, A. A. Fingelkurts, S. Bagnato, C. Boccagni, and G. Galardi, "EEG oscillatory states as neuro-phenomenology of consciousness as revealed from patients in vegetative and minimally conscious states," *Consciousness Cognition*, vol. 21, no. 1, pp. 149–169, Mar. 2012.
- [20] N. Jaworska, P. Blier, W. Fusee, and V. Knott, "Alpha power, alpha asymmetry and anterior cingulate cortex activity in depressed males and females," *J. Psychiatric Res.*, vol. 46, no. 11, pp. 1483–1491, Nov. 2012.
- [21] V. Knott, C. Mahoney, S. Kennedy, and K. Evans, "EEG power, frequency, asymmetry and coherence in male depression," *Psychiatry Res., Neuroimag.*, vol. 106, no. 2, pp. 123–140, Apr. 2001.
- [22] C. Nyström, M. Matousek, and T. Hällström, "Relationships between EEG and clinical characteristics in major depressive disorder," *Acta Psychiatrica Scandinavica*, vol. 73, no. 4, pp. 390–394, Apr. 1986.
- [23] A. A. Fingelkurts, A. A. Fingelkurts, H. Rytälä, K. Suominen, E. Isometsä, and S. Kähkönen, "Composition of brain oscillations in ongoing EEG during major depression disorder," *Neurosci. Res.*, vol. 56, no. 2, pp. 44–133, Oct. 2006.
- [24] J. J. B. Allen and S. J. Reznik, "Frontal EEG asymmetry as a promising marker of depression vulnerability: Summary and methodological considerations," *Current Opinion Psychol.*, vol. 4, pp. 93–97, Aug. 2015.
- [25] Y. Li, D. Cao, L. Wei, Y. Tang, and J. Wang, "Abnormal functional connectivity of EEG gamma band in patients with depression during emotional face processing," *Clin. Neurophysiol.*, vol. 126, pp. 2078–2089, Nov. 2015.
- [26] F. Sambataro, N. D. Wolf, M. Pennuto, N. Vasic, and R. C. Wolf, "Revisiting default mode network function in major depression: Evidence for disrupted subsystem connectivity," *Psychol. Med.*, vol. 44, no. 10, pp. 2041–2051, Jul. 2014.

- [27] T. Shen, C. Li, B. Wang, W. M. Yang, C. Zhang, Z. Wu, M. H. Qiu, J. Liu, Y. F. Xu, and D. H. Peng, "Increased cognition connectivity network in major depression disorder: A fMRI study," *Psychiatry Invest.*, vol. 12, no. 2, pp. 227–234, Apr. 2015.
- [28] X. Zhang, B. Hu, X. Ma, and L. Xu, "Resting-state whole-brain functional connectivity networks for MCI classification using L2-regularized logistic regression," *IEEE Trans. Nanobiosci.*, vol. 14, no. 2, pp. 237–247, Mar. 2015.
- [29] J. S. Anderson, J. A. Nielsen, A. L. Froehlich, M. B. DuBray, T. J. Druzgal, A. N. Cariello, J. R. Cooperrider, B. A. Zielinski, C. Ravichandran, P. T. Fletcher, A. L. Alexander, E. D. Bigler, N. Lange, and J. E. Lainhart, "Functional connectivity magnetic resonance imaging classification of autism," *Brain*, vol. 134, no. 12, pp. 3742–3754, Dec. 2011.
- [30] F. Liu, W. Guo, J.-P. Fouche, Y. Wang, W. Wang, J. Ding, L. Zeng, C. Qiu, Q. Gong, W. Zhang, and H. Chen, "Multivariate classification of social anxiety disorder using whole brain functional connectivity," *Brain Struct. Function*, vol. 220, no. 1, pp. 101–115, Jan. 2015.
- [31] T. T. Erguzel, S. Ozekes, O. Tan, and S. Gultekin, "Feature selection and classification of electroencephalographic signals: An artificial neural network and genetic algorithm based approach," *Clin. EEG Neurosci.*, vol. 46, no. 4, pp. 321–326, Oct. 2015.
- [32] B. Hosseiniard, M. H. Moradi, and R. Rostami, "Classifying depression patients and normal subjects using machine learning techniques and nonlinear features from EEG signal," *Comput. Methods Programs Biomed.*, vol. 109, no. 3, pp. 339–345, Mar. 2013.
- [33] W. Mumtaz, S. S. A. Ali, M. A. M. Yasin, and A. S. Malik, "A machine learning framework involving EEG-based functional connectivity to diagnose major depressive disorder (MDD)," *Med. Biol. Eng. Comput.*, vol. 56, pp. 233–246, Feb. 2018.
- [34] E. Schulz, A. Zherdin, L. Tiemann, C. Plant, and M. Ploner, "Decoding an individual's sensitivity to pain from the multivariate analysis of EEG data," *Cerebral Cortex*, vol. 22, no. 5, pp. 1118–1123, May 2011.
- [35] N. U. F. Dosenbach, B. Nardos, A. L. Cohen, D. A. Fair, J. D. Power, J. A. Church, S. M. Nelson, G. S. Wig, A. C. Vogel, C. N. Lessov-Schlaggar, K. A. Barnes, J. W. Dubis, E. Feczkó, R. S. Coalson, J. R. Pruett Jr., D. M. Barch, S. E. Petersen, and B. L. Schlaggar, "Prediction of individual brain maturity using fMRI," *Science*, vol. 329, no. 5997, pp. 1358–1361, 2010.
- [36] J. M. Garcia, J. R. Sirard, R. Larsen, M. Bruening, M. Wall, and D. Neumark-Sztainer, "Social and psychological factors associated with adolescent physical activity," *J. Phys. Activity Health*, vol. 13, no. 9, pp. 957–963, 2016.
- [37] A. Kemp, K. Griffiths, K. L. Felmingham, S. A. Shankman, W. Dringenburg, M. Arns, C. R. Clark, and R. A. Bryant, "Disorder specificity despite comorbidity: Resting EEG alpha asymmetry in major depressive disorder and post-traumatic stress disorder," *Biol. Psychol.*, vol. 85, no. 2, pp. 350–354, 2010.
- [38] A. F. Leuchter, I. A. Cook, A. M. Hunter, C. Cai, and S. Horvath, "Resting-state quantitative electroencephalography reveals increased neurophysiologic connectivity in depression," *PLoS ONE*, vol. 7, no. 2, 2012, Art. no. e32508.
- [39] J. Lee, J. Y. Hwang, S. M. Park, H. Y. Jung, S.-W. Choi, D. J. Kim, J.-Y. Lee, and J.-S. Choi, "Differential resting-state EEG patterns associated with comorbid depression in Internet addiction," *Prog. Neuropsychopharmacol. Biol. Psychiatry*, vol. 50, pp. 21–26, Apr. 2014.
- [40] Y. Noda, R. Zomorodi, T. Saeki, T. K. Rajji, D. M. Blumberger, Z. J. Daskalakis, and M. Nakamura, "Resting-state EEG gamma power and theta-gamma coupling enhancement following high-frequency left dorsolateral prefrontal rTMS in patients with depression," *Clin. Neurophysiol.*, vol. 128, no. 3, pp. 424–432, Mar. 2017.
- [41] C.-C. Chang and C.-J. Lin, "LIBSVM: A library for support vector machines," *ACM Trans. Intell. Syst. Technol.*, vol. 2, no. 3, p. 27, Apr. 2011.
- [42] K. Kroenke and R. L. Spitzer, "The PHQ-9: A new depression diagnostic and severity measure," *Psychiatric Ann.*, vol. 32, no. 9, pp. 509–515, Sep. 2002.
- [43] R. L. Spitzer, K. Kroenke, J. B. Williams, and B. Löwe, "A brief measure for assessing generalized anxiety disorder: The GAD-7," *Arch. Internal Med.*, vol. 166, no. 10, pp. 1092–1097, May 2006.
- [44] T. Walczak and S. Chokroverty, "Electroencephalography, electromyography and electrooculography: General principles and basic technology," in *Sleep Disorders Medicine*. Amsterdam, The Netherlands: Elsevier, 1994, pp. 95–117.
- [45] A. Widmann, E. Schröger, and B. Maess, "Digital filter design for electrophysiological data—A practical approach," *J. Neurosci. Methods*, vol. 250, pp. 34–46, Jul. 2015.
- [46] D. Yao, "A method to standardize a reference of scalp EEG recordings to a point at infinity," *Physiological Meas.*, vol. 22, no. 4, p. 693, Oct. 2001.
- [47] F. Mormann, K. Lehnhertz, P. David, and C. E. Elger, "Mean phase coherence as a measure for phase synchronization and its application to the EEG of epilepsy patients," *Phys. D, Nonlinear Phenomena*, vol. 144, nos. 3–4, pp. 358–369, Oct. 2000.
- [48] G. Nolte, O. Bai, L. Wheaton, Z. Mari, S. Vorbach, and M. Hallett, "Identifying true brain interaction from EEG data using the imaginary part of coherency," *Clin. Neurophysiol.*, vol. 115, no. 10, pp. 2292–2307, Oct. 2004.
- [49] C. J. Stam, G. Nolte, and A. Daffertshofer, "Phase lag index: Assessment of functional connectivity from multi channel EEG and MEG with diminished bias from common sources," *Hum. Brain Mapping*, vol. 28, no. 11, pp. 1178–1193, Nov. 2007.
- [50] L. L. Zeng, H. Shen, L. Liu, L. Wang, B. Li, P. Fang, Z. Zhou, Y. Li, and D. Hu, "Identifying major depression using whole-brain functional connectivity: A multivariate pattern analysis," *Brain*, vol. 135, pp. 1498–1507, May 2012.
- [51] M. Kendall and J. Gibbons, *Rank Correlation Methods*. New York, NY, USA: Oxford Univ. Press, 1990.
- [52] M. Ojala and G. C. Garriga, "Permutation tests for studying classifier performance," *J. Mach. Learn. Res.*, vol. 11, pp. 1833–1863, Jun. 2010.
- [53] S. Mukherjee, P. Golland, and D. Panchenko, "Permutation tests for classification," AI Memo 2003-019, Massachusetts Inst. Technol. Comput. Sci. Artif. Intell. Lab., Cambridge, MA, USA, 2003.
- [54] Y. I. Sheline, J. L. Price, Z. Yan, and M. A. Mintun, "Resting-state functional MRI in depression unmasks increased connectivity between networks via the dorsal nexus," *Proc. Nat. Acad. Sci. USA*, vol. 107, no. 24, pp. 11020–11025, 2010.
- [55] M. D. Greicius, B. H. Flores, V. Menon, G. H. Glover, H. B. Solvason, H. Kenna, A. L. Reiss, and A. F. Schatzberg, "Resting-state functional connectivity in major depression: Abnormally increased contributions from subgenual cingulate cortex and thalamus," *Biol. Psychiatry*, vol. 62, no. 5, pp. 429–437, Sep. 2007.
- [56] K. D. Young, G. J. Siegle, M. Misaki, V. Zotev, R. Phillips, W. C. Drevets, and J. Bodurka, "Altered task-based and resting-state amygdala functional connectivity following real-time fMRI amygdala neurofeedback training in major depressive disorder," *NeuroImage, Clin.*, vol. 17, pp. 691–703, Dec. 2018.
- [57] C. Tas, M. Cebi, O. Tan, G. Hizli-Sayar, N. Tarhan, and E. C. Brown, "EEG power, cordance and coherence differences between unipolar and bipolar depression," *J. Affect. Disorders*, vol. 172, pp. 184–190, Feb. 2015.
- [58] C. G. Connolly, J. Wu, T. C. Ho, F. Hoeft, O. Wolkowitz, S. Eisendrath, G. Frank, R. Hendren, J. E. Max, M. P. Paulus, S. F. Tapert, D. Banerjee, A. N. Simmons, and T. T. Yang, "Resting-state functional connectivity of subgenual anterior cingulate cortex in depressed adolescents," *Biol. Psychiatry*, vol. 74, no. 12, pp. 898–907, Dec. 2013.
- [59] E. Alalade, K. Denny, G. Potter, D. Steffens, and L. Wang, "Altered cerebellar-cerebral functional connectivity in geriatric depression," *Plos ONE*, vol. 6, no. 5, 2011, Art. no. e20035.
- [60] A. A. Fingelkurt, A. A. Fingelkurt, H. Rytsälä, K. Suominen, E. Isometsä, and S. Kähkönen, "Impaired functional connectivity at EEG alpha and theta frequency bands in major depression," *Hum. Brain Mapping*, vol. 28, no. 3, pp. 247–261, 2007.
- [61] L. L. Zeng, H. Shen, L. Liu, and D. Hu, "Unsupervised classification of major depression using functional connectivity MRI," *Hum. Brain Mapping*, vol. 35, no. 4, pp. 1630–1641, Apr. 2014.
- [62] D. A. Pizzagalli, T. R. Oakes, and R. J. Davidson, "Coupling of theta activity and glucose metabolism in the human rostral anterior cingulate cortex: An EEG/PET study of normal and depressed subjects," *Psychophysiology*, vol. 40, no. 6, pp. 939–949, Nov. 2003.
- [63] C. Muler, G. Juckel, M. Brunnmeier, S. Karch, G. Leicht, R. Mergl, H. J. Möller, U. Hegerl, and O. Pogarell, "Rostral anterior cingulate cortex activity in the theta band predicts response to antidepressive medication," *Clin. EEG Neurosci.*, vol. 38, no. 2, pp. 78–81, Apr. 2007.
- [64] J. C. Mosher and R. M. Leahy, "Recursive Music: A framework for EEG and MEG source localization," *IEEE Trans. Biomed. Eng.*, vol. 45, no. 11, pp. 1342–1354, Nov. 1998.
- [65] R. D. Pascual-Marqui, "Standardized low-resolution brain electromagnetic tomography (sLORETA): Technical details," *Methods Find Exp. Clin. Pharmacol.*, vol. 24, pp. 5–12, Jan. 2002.